ChemComm

COMMUNICATION

View Article Online
View Journal | View Issue

Cite this: *Chem. Commun.*, 2014, **50**, 7720

Received 6th May 2014,
Accepted 28th May 2014

DOI: 10.1039/c4cc03409k

www.rsc.org/chemcomm

A new class of organic photovoltaic materials: poly(rod-coil) polymers having alternative conjugated and non-conjugated segments†

Hong-Jiao Li, Jin-Tu Wang, Chong-Yu Mei and Wei-Shi Li*

A new class of organic photovoltaic materials, poly(rod-coil) polymers composed of alternatively definite conjugated and non-conjugated segments, have been proposed. The first five examples based on polyurethane chemistry showed photovoltaic performance surpassing the reference compound, but less dependent on their molecular weight.

Over the past decade, remarkable achievement has been made in organic photovoltaic donor materials, which substantially improved the power conversion efficiency (PCE) of organic solar cells (OSCs).[1] The so far reported donor materials can be categorized into two main classes: π-conjugated polymers[1,2] and small molecular compounds.[1,3] Conjugated polymers have a one-dimensional π-conjugated backbone, which is favourable for light acquisition and the transportation of excitons and charge carriers. Besides, polymer materials generally have a good film formation potential and are adaptable to various solution processing technologies. However, all polymers have issues of average molecular weight and polydispersity, which always vary from batch to batch. Since their photovoltaic properties are sensitive to these parameters,[4] conjugated polymers usually suffer from poor batch-reproducibility, a severe problem for their real applications. On the other hand, small molecular compounds do not have such problems since they have a definite chemical structure and can be purified by means of many well-developed techniques. However, for the purpose of promising light absorption and good charge transportation, these kinds of compounds usually have a large and rigid π-conjugated core. Consequently, they tend to aggregate or crystallize, and are hard to form a well-qualified homogenous film, particularly in a large size.

Herein, we propose a new class of polymeric photovoltaic materials with a structural feature in-between conventional conjugated polymers and small molecular compounds. As illustrated in Scheme 1a, this class of materials are poly(rod-coil) polymers composed of definite conjugated and non-conjugated segments in an alternative fashion. Conjugated rigid segments are photo-active and basically determine optoelectronic properties of the material. For photovoltaic application, these segments are suggested to be made of donor–acceptor (D–A) and related structures for efficient light harvesting.[1–3] Since they have definite chemical structures, like conventional photovoltaic compounds, the final material would possess a performance less sensitive to its molecular weight and polydispersity. Furthermore, owing to their polymeric nature, good film formation potential could be expected for these kinds of materials.

In this contribution, we report the first set of examples based on well-known polyurethane chemistry. Firstly, we synthesized compound **DPP(3TPOH)$_2$** bearing one hydroxyl unit at both ends and a diketopyrrolopyrrole-centred D–A–D conjugated moiety[5] (Scheme 1b and ESI†). Secondly, **DPP(3TPOH)$_2$** was copolymerized with various diisocyanate monomers, including hexamethylene diisocyanate, 1,4-phenylene diisocyanate, 1,3-phenylenediisocyanate, and methylene-diphenyl 4,4′-diisocyanate, producing four kinds of polyurethane polymers named **PU1**, **PU2**, **PU3**, and two **PU4** (**PU4**-LW and **PU4**-HW) with different molecular weight, respectively. The average number molecular weight (M_n) and polydispersity index (PDI) were determined to be 4.12 kDa and 1.08 for **PU1**, while 6.40 kDa and 1.15 for **PU2**, 6.66 kDa and 1.40 for **PU3**, 7.90 kDa and 1.39 for **PU4**-LW, and 16.7 kDa and 1.94 for **PU4**-HW. Obviously, **PU1**, **PU2**, **PU3** and **PU4**-LW have comparable molecular weight, while M_n of **PU4**-HW is doubled. Meanwhile, compound **DPP(3TP)$_2$** with saturated alkyl end chains was prepared as a small molecular reference compound for comparison.

Compared with **DPP(3TP)$_2$**, polymers **PU1**, **PU2**, **PU3** and **PU4** have different thermal properties and solid-state structures. Thermogravimetric analysis (TGA, Fig. S10, ESI†) revealed that these polymers have a 5%-weight-loss decomposition temperature (T_d) in the range of 258–298 °C, lower than **DPP(3TP)$_2$** (383 °C). In the differential scanning calorimetry (DSC, Fig. S11, ESI†), only a glass transition around 60 °C and an weak endothermic peak at 160 °C were observed for **PU3** and **PU4** in the second heating procedure, while three small peaks at around 88, 101, and 187 °C for **PU2**.

Laboratory of Synthetic and Self-Assembly Chemistry for Organic Functional Molecules, Shanghai Institute of Organic Chemistry, Chinese Academy of Sciences, 345 Lingling road, Shanghai 200032, China. E-mail: liws@mail.sioc.ac.cn

† Electronic supplementary information (ESI) available: Materials and synthesis, TGA, DSC, XRD, UV, CV, TEM, and OSC device optimization. See DOI: 10.1039/c4cc03409k

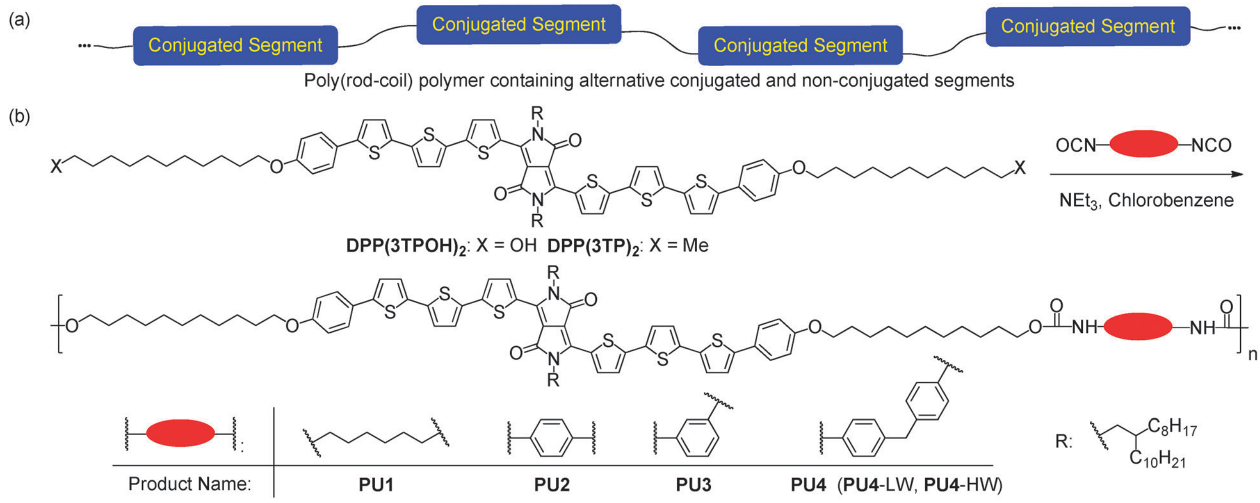

Scheme 1 (a) Schematic representation of proposed poly(rod-coil) photovoltaic polymers. (b) Synthesis of photovoltaic polyurethanes.

In sharp contrast, a couple of intense phase transition peaks (51, 102, 138 and 176 °C) appeared in the second heating DSC trace of **DPP(3TP)$_2$**. Especially, the endothermic enthalpy for the peak at 138 °C is extremely large, suggesting that **DPP(3TP)$_2$** is a crystalline material. X-ray diffraction analysis (XRD, Fig. S12, ESI†) further confirmed that **DPP(3TP)$_2$** is crystalline at room temperature while **PU2–PU4** is amorphous. Although a sharp phase transition was observed at around 115 °C together with a weak one at around 155 °C for the **PU1** polymer, the non-structured XRD profile indicates that it is also an amorphous material at room temperature.

Fig. 1 displays UV-vis absorption spectra of the polymers and the reference compound in both solution and film states. In chloroform solution, all the polymers exhibited a similar electronic absorption spectrum to **DPP(3TP)$_2$**, with two featured bands in the regions of 300–500 nm and 500–750 nm for π–π* and intramolecular charge transfer (ICT) transition, respectively (Fig. 1a).[6] It is valuable to point out that the two peaks at around 622 and 654 nm observed for the ICT band of **DPP(3TP)$_2$** are due to the vibronic progression since they did not change upon dilution (Fig. S13, ESI†). In the film state, **PU2–PU4** displayed a new intense peak in the range of 705–714 nm in addition to their 10–19 nm-red-shifted ICT bands (Fig. 1b). This suggests the occurrence of strong π–π interactions among the conjugated segments in the film state. In comparison, **DPP(3TP)$_2$** only showed a relatively weak shoulder at this region, indicating that its film structure is not favourable for π–π interactions among the molecules. For **PU1** polymer film, an ICT band (606 nm) blue-shifted to that in solution (630 nm), together with a weak shoulder at 708 nm, was observed, suggesting the formation of a different aggregation style, probably H-aggregates. Although the differences were observed in the absorption peaks, the film state absorption spectra of either polymers or **DPP(3TP)$_2$** displayed the same onset point at around 780 nm, giving an energy band gap of 1.59 eV for all the materials. Cyclic voltammetry further confirmed that all the materials have a similar highest occupied molecular orbital (HOMO) energy level at −5.3 eV (Fig. S14, ESI†). These results indicate the change from small molecules to polymers and the different urethane linkers, as well as polymer molecular weight, do not alter many basic optoelectronic properties of the materials, such as absorption bands in solution, energy band gap and molecular orbital energy levels, but does affect the aggregation-induced properties of the materials.

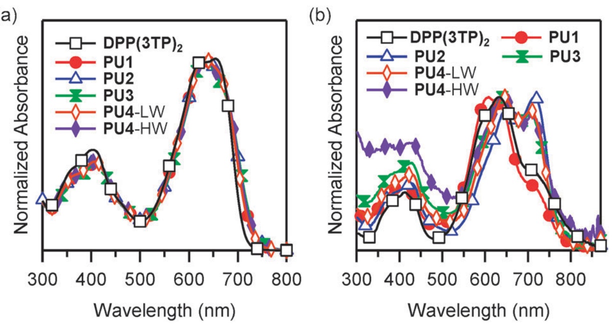

Fig. 1 Normalized UV-vis absorption spectra of **DPP(3TP)$_2$**, **PU1**, **PU2**, **PU3**, **PU4**-LW and **PU4**-HW in chloroform solutions with a concentration of 1×10^{-5} M (a) and in film state (b).

Bulk heterojunction OSCs with a conventional structure of ITO/PEDOT:PSS/active layer/Al using the synthesized polymers and **DPP(3TP)$_2$** as donor components while [6,6]-phenyl-C$_{61}$-butyric acid methyl ester (PC$_{61}$BM) as the acceptor component were fabricated. It was found that the best weight ratio of donor/PC$_{61}$BM varied with the checked donor materials, in which 1 : 2 for **DPP(3TP)$_2$**, 1 : 3 for **PU3**, 1 : 5 for **PU4**-LW, while 1 : 4 for the rest of the polyurethanes (Tables S1–S6, ESI†). Other fabrication conditions, including solvent, concentration, the spin-coating rate, annealing temperature, and the addition of 1,8-diiodooctane (DIO), were also optimized. Fig. 2 displays the device performance of all the checked systems under their respective optimized conditions, while their parameters are summarized in Table 1. From these data, one can find that all the polymers under optimized conditions displayed improved photovoltaic performance compared to **DPP(3TP)$_2$** with an increasing factor of 29–73%.

Detailed comparison showed that the change from **DPP(3TP)$_2$** to the polymers did not alter open-circuit voltage (V_{OC}) and short-circuit

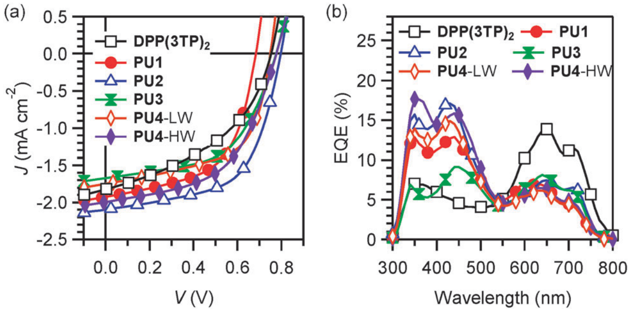

Fig. 2 (a) *J*–*V* curves under AM 1.5 G illumination with a density of 100 mW cm^{-2} and (b) EQE spectra of the best OSCs based on **DPP(3TP)$_2$**, **PU1**, **PU2**, **PU3**, **PU4**-LW and **PU4**-HW as donor component while PC$_{61}$BM as acceptor components under the optimized conditions shown in Tables S1–S6 (ESI†).

Table 1 Device parameters of the organic solar cells shown in Fig. 2

Donor	V_{OC} (V)	J_{SC} [a] (mA cm^{-2})	FF (%)	PCE [b] (%)	μ_h (cm^2 V^{-1} s^{-1})	μ_e (cm^2 V^{-1} s^{-1})
DPP(3TP)$_2$	0.76	1.82 (1.98)	43.2	0.59 (0.55)	1.3×10^{-4}	5.6×10^{-4}
PU1	0.68	1.92 (1.62)	57.0	0.75 (0.71)	1.4×10^{-4}	1.8×10^{-5}
PU2	0.80	2.09 (1.87)	58.8	0.98 (0.95)	1.8×10^{-5}	2.5×10^{-5}
PU3	0.77	1.67 (1.49)	55.1	0.71 (0.68)	6.1×10^{-5}	1.5×10^{-4}
PU4-LW	0.75	1.75 (1.57)	58.4	0.77 (0.76)	4.7×10^{-5}	5.8×10^{-4}
PU4-HW	0.78	1.99 (1.78)	53.0	0.82 (0.77)	6.0×10^{-5}	2.1×10^{-4}

[a] Data in parentheses are the J_{SC} values calculated from EQE spectra shown in Fig. 2b. [b] Data in parentheses are the average values.

current (J_{SC}) a lot although in some cases a slight enhancement or reduction was observed. This can be well understood since the opto-electronically active segments for all the polymers are the same as that of **DPP(3TP)$_2$** and all polymers do possess a similar HOMO energy level like **DPP(3TP)$_2$**. As for J_{SC}, external quantum efficiency (EQE) spectroscopy revealed the photocurrent of the polymer-based cells decreased in the range of 550–750 nm but increased in the range of 300–550 nm (Fig. 2b). These two sides compensated each other and thus resulted in comparable J_{SC} values. Therefore, the performance improvement of the polymer-based solar cells finally came from the enhancement in the FF value, which increased from 43.2% for the **DPP(3TP)$_2$**-based cell to over 53% for the polymer-based ones. When the comparison was carried out among the polymer blend films, one could easily find that **PU2** showed the best photovoltaic output with a PCE of nearly 1%. More importantly, the optimized solar cell based on **PU4**-LW or **PU4**-HW having a large difference in molecular weight displayed comparable performance. This result verified our initial expectation that the molecular weight has less influence on the photovoltaic properties for this new class of photovoltaic polymers and would be a merit for their real applications.

In order to investigate the origin of the performance difference, the morphology and charge transportation of the blend films for the best devices were studied. As revealed by transmission electron microscopy (Fig. S15, ESI†), the **DPP(3TP)$_2$**/PC$_{61}$BM blend film presented a large island-sea phase separation microstructure, while those of polymer blend films appeared to be homogeneous without clear phase separation. Obviously, the latter is favourable to device performance since it could provide much smaller phase domains and a larger heterojunction interface. On the other hand, the mobility measurements by the space-charge-limited method indicate that the **DPP(3TP)$_2$**/PC$_{61}$BM blend film possesses hole and electron mobilities larger than most of the polymer blend films, but comparable to some cases (Table 1). These results obviously suggest that the morphology change would be the main reason for the above-mentioned performance improvement observed for the polymers.

In summary, we have demonstrated a new class of polymeric photovoltaic materials, which contain multiple conjugated rigid segments but linked by non-conjugated soft chains. Compared with their small molecular reference, the present five photovoltaic polyurethane examples exhibited the performance improvement by a factor of 29–73%. Moreover, the molecular weight seems no longer to be one of the important factors that affect the material properties. Although PCE in the present examples is low, this work opens an avenue for the development of new photovoltaic materials with the features of both small molecular compounds and polymers. For improving the performance of these kinds of materials, there are a lot of things that can be done, for example, well design and optimization either of the opto-electronically active segments, or the non-conjugated soft linking segments, including the type of linking functionalities and pattern, the nature and length of linking chains. Furthermore, this material design strategy is not only limited to the OPV materials, but also can be applied in the fields of organic field-effect transistors and organic light-emitting diodes.

We gratefully acknowledge the financial support from the National Natural Science Foundation of China (No. 20974119, 90922019, and 21074147), Shanghai Science and Technology Commission (No. 13JC1407000), and Chinese Academy of Sciences.

Notes and references

1 For selected recent reviews, see: (*a*) Y.-J. Cheng, S.-H. Yang and C.-S. Hsu, *Chem. Rev.*, 2009, **109**, 5868; (*b*) P. M. Beaujuge and J. M. J. Fréchet, *J. Am. Chem. Soc.*, 2011, **133**, 20009; (*c*) H. Zhou, L. Yang and W. You, *Macromolecules*, 2012, **45**, 607; (*d*) G. Li, R. Zhu and Y. Yang, *Nat. Photonics*, 2012, **6**, 153; (*e*) L. Dou, J. You, Z. Hong, Z. Xu, G. Li, R. A. Street and Y. Yang, *Adv. Mater.*, 2013, **25**, 6642; (*f*) A. J. Heeger, *Adv. Mater.*, 2014, **26**, 10.

2 (*a*) P.-L. T. Boudreault, A. Najari and M. Leclerc, *Chem. Mater.*, 2011, **23**, 456; (*b*) H. Ye, W. Li and W.-S. Li, *Chin. J. Org. Chem.*, 2012, **32**, 266.

3 (*a*) A. Mishra and P. Bäuerle, *Angew. Chem., Int. Ed.*, 2012, **51**, 2020; (*b*) Y. Lin, Y. Li and X. Zhan, *Chem. Soc. Rev.*, 2012, **41**, 4245.

4 (*a*) J. C. Bijleveld, A. P. Zoombelt, S. G. J. Mathijssen, M. M. Wienk, M. Turbiez, D. M. de Leeuw and R. A. J. Janssen, *J. Am. Chem. Soc.*, 2009, **131**, 16616; (*b*) R. S. Ashraf, B. C. Schroeder, H. A. Bronstein, Z. Huang, S. Thomas, R. J. Kline, C. J. Brabec, P. Rannou, T. D. Anthopoulos, J. R. Durrant and I. McCulloch, *Adv. Mater.*, 2013, **25**, 2029; (*c*) J. Wang, H. Ye, H. Li, C. Mei, J. Ling, W. Li and Z. Shen, *Chin. J. Chem.*, 2013, **31**, 1367.

5 (*a*) S. Qu and H. Tian, *Chem. Commun.*, 2012, **48**, 3039; (*b*) C. B. Nielsen, M. Turbiez and I. McCulloch, *Adv. Mater.*, 2013, **25**, 1859.

6 B. P. Karsten and R. A. J. Janssen, *Macromol. Chem. Phys.*, 2011, **212**, 515.